

Hydrogen in ZnO revisited: Bond center versus antibonding site

Xian-Bin Li,¹ Sukit Limpijumnong,^{2,3,*} Wei Quan Tian,⁴ Hong-Bo Sun,¹ and S. B. Zhang^{1,2,5}

¹State Key Laboratory on Integrated Optoelectronics, College of Electronic Science and Engineering, Jilin University, Changchun 130012, People's Republic of China

²National Renewable Energy Laboratory, Golden, Colorado 80401, USA

³School of Physics, Suranaree University of Technology and National Synchrotron Research Center, Nakhon Ratchasima 30000, Thailand

⁴State Key Laboratory of Theoretical and Computational Chemistry, Institute of Theoretical Chemistry, Jilin University, Changchun 130023, People's Republic of China

⁵Department of Physics, Applied Physics, and Astronomy, Rensselaer Polytechnic Institute, Troy, New York 12180, USA

(Received 13 August 2008; published 15 September 2008)

Current controversy on the binding sites of H^+ in ZnO can be explained by first-principles calculations.

Previous infrared measurements from different groups indicate different H sites, either at the bond center (BC) site with a stretch frequency $\omega=3611\text{ cm}^{-1}$ or antibonding (AB) site with $\omega=3326\text{ cm}^{-1}$. This was puzzling because the BC site has lower energy by 0.2 eV. Here, we show that calcium, isovalent to Zn and found only in samples with the 3326 cm^{-1} mode, binds H at the AB site. Large spatial undulation of charge explains the unexpected large binding between isovalent Ca and charged H^+ of 0.7 eV.

DOI: 10.1103/PhysRevB.78.113203

PACS number(s): 61.72.Bb, 63.20.Pw

Hydrogen in ZnO has attracted a lot of attention in the last decade. In 2000, Van de Walle proposed that H prefers to form a strong O-H bond with lattice O and acts exclusively as a donor, H^+ .¹ This behavior is different from H in almost all other semiconductors in which H is amphoteric, counteracting the dominant dopant.² ZnO is a potential superior electronic material for next-generation blue optoelectronic applications. However, due to the lacking of high quality *p*-type samples, fabrication of ZnO-based optoelectronic devices is still not possible. The prediction that H is an exclusive donor stirred up considerable research activities because it may explain the difficulty in *p* doping.^{3–11}

Binding site is one of the most fundamental properties of any impurity. Although it is clear that H^+ prefers to bind strongly with O at a bond length of approximately 1 Å and with a vibration frequency around 3500 cm^{-1} , the details are completely controversial: McCluskey *et al.*⁶ observed an IR peak at 3326 cm^{-1} in samples provided by Cermet, while Lavrov *et al.*¹² observed a different peak at 3611 cm^{-1} in samples by Eagle-Picher. Polarized IR showed that the 3326 cm^{-1} peak is associated with an oscillator orientated at 112° angle with respect to the *c* axis, whereas those that give the 3611 cm^{-1} peak are parallel to the axis. Later study by Shi *et al.*⁷ on both samples showed that the Cermet samples have a strong 3326 cm^{-1} peak and a weak 3611 cm^{-1} peak but the Eagle-Picher samples do exactly the opposite. This indicates that there exist two forms of O-H in these two types of samples. Because the splitting $3611-3326=285\text{ cm}^{-1}$ is comparable to the calculated splitting between the BC and AB site adjacent to O (AB_O), the 3611 cm^{-1} peak has been assigned to $BC_{||}$ and the 3326 cm^{-1} peak to $AB_{O\perp}$,¹³ where $||$ and \perp denote the orientation of the O-H bond with respect to the *c* axis [see Fig. 1(a)].

However, independent calculations by different groups^{12,13} showed consistently that the $BC_{||}$ site has lower formation energy than any other site by 0.2 eV, which, in comparison with the experimental temperature of 4 K, is quite large. More importantly, it is difficult to understand why the $AB_{O\perp}$ configuration can dominate in some samples

but not in others. An alternative explanation is that one (or both) of the signals may come from an H complex rather than just an isolated H^+ . Recently, McCluskey and Jokela¹⁴ studied the trace-amount elements in both samples by using delayed gamma neutron activation analysis (DGNAA) and secondary-ion mass spectrometry (SIMS). They found that the Cermet samples, grown by a pressurized melt-growth

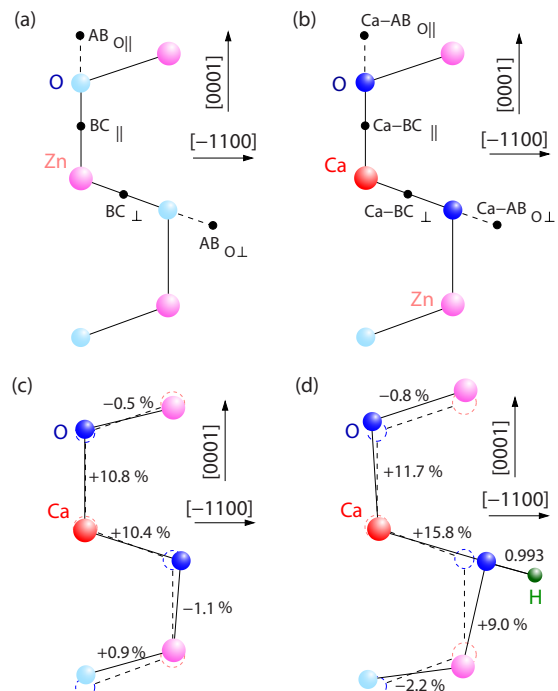


FIG. 1. (Color online) [(a) and (b)] Schematics in the (11–20) plane of the four H^+ sites in Ca-free ZnO and near a Ca impurity. Calculated atomic relaxations of Ca- $AB_{O\perp}$ (c) in the absence and (d) in the presence of H^+ . Oxygen atoms adjacent to the Ca are marked by darker blue. Dashed circles and dashed lines indicate the original bulk positions and bonds. Distances are given either in unit of angstrom or in percentage with respect to that of bulk ZnO.

TABLE I. Calculated formation energy, O-H bond length, and stretch frequencies for H⁺ in ZnO without (upper panel) and with (lower panel) Ca. The energy zero is that of Ca-free BC_{||} site. Highlighted rows are the ground-state configurations.

Site	ΔE (eV)		$d_{\text{O-H}}$ Å		Vibration frequency, ω (cm ⁻¹)		
	Present	Ref. 13	Present	Ref. 13	Present	Ref. 13	Measured
BC	0.00	0.00	0.985	0.986	3421	3475	3611^a
BC _⊥	0.14	0.15	0.985	0.982	3505	3519	
AB _O	0.19	0.17	1.001	1.003	3097	3116	
AB _{O⊥}	0.15	0.14	1.004	1.003	3109	3154	
Ca-BC	0.54		0.967		3934		
Ca-BC _⊥	0.38		0.979		3484		
Ca-AB _O	-0.29		0.995		3236		
Ca-AB _{O⊥}	-0.49		0.993		3207		3326^b

^aReference 12.

^bReference 6.

process,¹⁵ contain isovalent Ca impurity, whereas in the Eagle-Picher samples, which were grown by chemical vapor transport,¹⁶ the amount of Ca impurity is below the detection threshold.

In this Brief Report, we show that Ca may play a pivotal role in switching the H from the BC_{||} site to the AB_{O⊥} site. Our calculation shows that, with Ca, the AB_{O⊥} site is 0.5 eV more stable than the ground-state BC_{||} site in pure, Ca-free ZnO. Our results are consistent with the experimental finding that, for Cermet samples with Ca, the 3326 cm⁻¹ line is observed with the transition moment aligned at 112° from the *c* axis, whereas for Eagle-Picher samples without Ca, the 3611 cm⁻¹ line with a transition moment aligned along the *c* axis is observed. The fact that an isovalent impurity can bind H⁺ so strongly by 0.5+0.2=0.7 eV is unexpected and hence surprising. Our analysis shows that this could be a general property of ionic semiconductors and solids for which the electrostatic monopole (such as H⁺) and dipole (due to spatial undulated local field) interactions can be comparable to the monopole-monopole interactions (such as within a donor-acceptor pair) in more covalent materials.

We used the density-functional theory¹⁷ within the local-density approximation (LDA) and the projector augmented wave method^{18,19} as implemented in the VASP code.^{20,21} Zinc 3d states are treated as valence states. The cut-off energy for the plane-wave expansion is 400 eV. We used a supercell approach (96-atom wurtzite cell) with the Monkhorst-Pack *k*-point mesh for the Brillouin-zone integration ($2 \times 2 \times 2$). For charged defect, we used the jellium background approximation. All the atoms are allowed to relax to their equilibrium positions. To calculate the O-H frequencies, we employed the approach in Ref. 13 to include anharmonic effects. For free H₂O molecule, this yields a symmetric stretch frequency of 3540 cm⁻¹, which is lower than experiment²² by $\omega_{ER}=117$ cm⁻¹ (an error of $\sim 3\%$). To correct such a systematic error, ω_{ER} has been added to all the calculated results before comparing with experiments.

Table I shows the calculated formation energies ΔE [relative to the ground-state (BC_{||}) energy in Ca-free ZnO], O-H bond lengths $d_{\text{O-H}}$, and stretch frequencies ω for H⁺ in ZnO

without Ca (upper panel) and with Ca (lower panel). To be consistent, the upper panel are the results of current 96-atom cell calculations, which are qualitatively the same as previous calculations, e.g., $d_{\text{O-H}}$ and ω agree with our previous results to within 1% and 3%, respectively.¹³ With Ca, we denote the complexes as Ca-BC_{||}, Ca-BC_⊥, Ca-AB_{O||}, and Ca-AB_{O⊥}, respectively, with their atomic structures schematically shown in Fig. 1(b). The formation energies of the Ca-containing complexes are defined as

$$\Delta E = E_{\text{tot}}(\text{Ca} - \text{H}^+) + E_{\text{tot}}(\text{bulk}) - E_{\text{tot}}(\text{Ca}_{\text{Zn}}) - E_{\text{tot}}(\text{BC}_{||}), \quad (1)$$

where $E_{\text{tot}}(\alpha)$ is the total energy of a supercell containing the complex (or impurity) α . Physically, ΔE is the energy gain or loss by bringing a H⁺ from the lowest-energy BC_{||} site in Ca-free ZnO to the respective sites near the Ca in Fig. 1(b). A negative ΔE implies that the H⁺ is bounded, whereas a positive ΔE implies that the H⁺ is unbounded, to the Ca. Even when ΔE is positive, the site is still metastable due to the diffusion barriers of H⁺ in ZnO.

As Ca is *isovalent* to Zn, on a first look, it is puzzling why a charged H⁺ would like to bind to a neutral Ca with a rather sizable energy—a behavior usually found either in oppositely charged donor-acceptor pairs or in charge neutral but large-strain compensated defect pairs. Our calculation shows that both substitutional Ca and interstitial H⁺ cause outward relaxations to the surrounding Zn and O atoms. Therefore, neither of the above can be the cause for the unusually large binding energy. It is even more puzzling why the site preference is reversed from the BC site to the AB_O sites.

To understand the puzzles, we note first that H⁺ in ZnO binds to the oxygen atoms rather than any of the cation atoms. Second, ZnO is a highly ionic semiconductor with an ionicity of 0.616 in Phillips' scale.²³ In other words, although ideal ZnO is a homogeneous bulk material, there is a large spatial undulation of the electric field at the atomic level. Therefore, the defect and impurity physics that is already well established for covalent semiconductors such as Si or GaAs may not necessarily apply here. Rather, it is how much

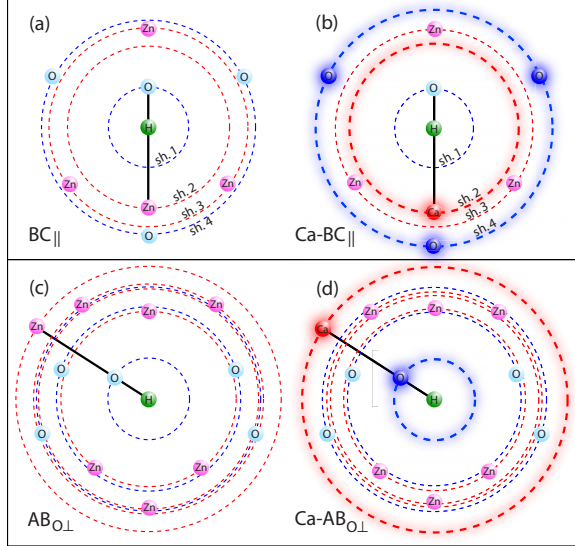


FIG. 2. (Color online) Radial distributions of neighboring atoms surrounding an H⁺ at different sites: (a) BC_{||}, (b) Ca-BC_{||}, (c) AB_{O⊥}, and (d) Ca-AB_{O⊥}. Solid lines highlight the local bonds: O-H-Zn (or O-H-Ca) for the BC sites and H-O-Zn (or H-O-Ca) for the AB_O sites. Dashed circles indicate the radial distances from the H⁺ center. For simplicity, atoms in the shell are evenly distributed. In (b) and (d), shells with enhanced charge with respect to (a) and (c) are highlighted by halo: blue for enhanced negative and red for enhanced positive.

the impurity affects the undulation of the field that holds the key to defect and impurity physics in ionic semiconductors. The electronegativity of Ca, Zn, and O, on the Pauling scale, is $\chi^{\text{Ca}}=1.00$, $\chi^{\text{Zn}}=1.65$, and $\chi^{\text{O}}=3.44$. Therefore, Ca has a stronger tendency to donate its electrons to neighboring O atoms than Zn does. This stronger charge transfer makes the O atoms adjacent to the Ca atom stronger negative centers relative to other O atoms. As such, qualitatively speaking, the H⁺ should bind to these O atoms more strongly. Also, because Ca is a much stronger positive charge center than Zn, a H⁺ would avoid the BC sites adjacent to Ca, making the adjacent AB_O sites energetically more favorable.

To further the discussion, next we apply a Bader analysis.^{24,25} Our calculations show that in bulk ZnO, each Zn donates 1.13 electrons to O. In other words, Zn can be considered as a positive center with $q=+1.13e$ whereas O can be considered as a negative center with $q=-1.13e$. This explains why an H⁺ prefers to stay close to the O, instead of Zn. Bader analysis of Ca_{Zn} further shows that Ca donates 1.42e, which is 0.29e more than what Zn does. The extra donation is almost equally distributed among the four O nearest neighbors: 0.06e to the O in the [0001] direction, and 0.07e to each of the remaining three O.

To understand the switching in site preference from BC in bulk ZnO to AB_O near Ca_{Zn}, we need to examine next-nearest neighbors ($\sim 2 \text{ \AA}$) where the difference between the BC and AB_O sites can be readily seen. Figure 2 shows, in a schematic shell model, the radial distributions of neighboring atoms of H. It so happens that before introducing the Ca, the four sites in the upper panel of Table I, BC_{||}, BC_⊥, AB_{O||}, and AB_{O⊥}, have reasonably close formation energies to within

0.2 eV. This enables us to interpret the changes upon Ca substitution primarily in terms of a *redistribution* of the charge. Because the BC sites are closer to the Ca [e.g., Fig. 2(b)], they become energetically unfavorable. In contrast, the AB_O sites are much further away from the Ca [see, Fig. 2(d)]. As a result, the AB_O sites benefit more from the charge redistribution, forming a stronger O-H⁺ bond yet staying away from the positive Ca so as not to be strongly affected by it. Moreover, because H in the BC sites cuts the Ca-O bonds, it effectively blocks charge transfer from Ca to O. As a matter of fact, Bader charge on the first shell O atom in Fig. 2(b) is the same as the Ca-free case. Hence, not only does the Ca-BC sites become less favorable than the Ca-AB_O sites, the formers are positive in energy with respect to the BC_{||} site away from the Ca. In other words, H⁺ will not bind to the Ca at the Ca-BC sites.

Next, we estimate the equilibrium distribution of H⁺ among the various lattice sites α . By constructing the partition functions, we can derive the equations relating the concentration of H⁺(α), [H⁺(α)], to the overall chemical potential of H⁺, μ_{H^+} .²⁶ Because we consider only H⁺, Fermi-level dependence of the various sites α is the same. Vibrational energy contributions for these sites are similar, as well. Their contributions can thus be expressed as E_0 and

$$\tilde{\mu}_{\text{H}^+} = \mu_{\text{H}^+} - E_0 = \Delta E(\alpha) + kT \ln \left\{ \frac{[\text{H}^+(\alpha)]}{j(n(\alpha) - [\text{H}^+(\alpha)])} \right\}, \quad (2)$$

where $\Delta E(\alpha)$ is the formation energy of H⁺(α) in Table I, $n(\alpha)$ is the density of available lattice sites for a specific H⁺(α), and j is the number of symmetry degeneracy. For example, for H⁺ at BC_{||} site, we have $\mu_{\text{H}^+}=0.0 \text{ eV} + kT \ln\{[\text{H}^+(\text{BC}_{||})]/[\text{O}]-[\text{H}^+(\text{BC}_{||})]\}$, and for H⁺ at Ca-AB_{O⊥} site, we have $\tilde{\mu}_{\text{H}^+}=-0.49 \text{ eV} + kT \ln\{[\text{H}^+(\text{Ca-AB}_{O\perp})]/3[\text{Ca}]-[\text{H}^+(\text{Ca-AB}_{O\perp})]\}$. To solve the set of equations, we apply the equilibrium constraint that $\tilde{\mu}_{\text{H}^+}$ is the same for all the H⁺(α). We also require that the total concentration of H⁺ satisfies $[\text{H}^+] = \sum [\text{H}^+(\alpha)]$, whose value is an input from experimental conditions.

For Cermet samples, the concentration of Ca is measured to be $[\text{Ca}]=4 \times 10^{16} \text{ cm}^{-3}$ (Ref. 14) and the total concentration of H⁺ is expected to be at most in the same order of magnitude (so we use $[\text{H}^+]=4 \times 10^{16}$ for the illustration purpose). Figure 3(a) shows the normalized equilibrium concentrations as a function of temperature. Concentrations with less than 5% of total [H⁺] are ignored in the figure. We see that the majority (over 75%) of H⁺ is on the Ca-AB_{O⊥} sites for temperatures below 400 K (or 127 °C). It has been predicted that H⁺ diffuses readily at room temperature due to its low migration barrier of less than 0.5 eV (Refs. 3 and 27) to equilibrate the H⁺ among the various lattice sites. For Eagle-Picher samples, the concentration of Ca is outside experimental detection limit and is hence much less than that of H⁺. Figure 3(b) shows the results for such a case. Here as expected, the majority (over 75%) of H⁺ is on the BC_{||} sites for temperatures less than 600 K.

The calculated vibrational signatures of the H⁺ sites are also in agreement with experiments. For example, the stretch

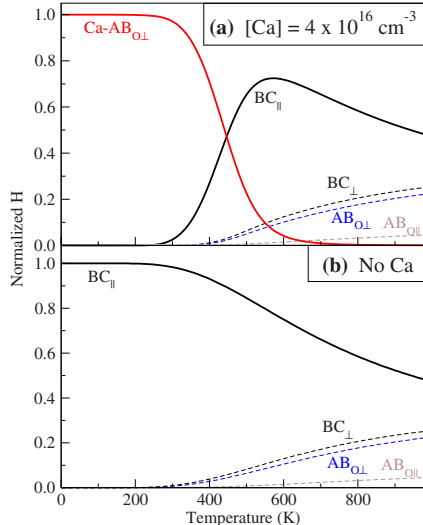


FIG. 3. (Color online) Normalized equilibrium concentrations of $[H^+(\alpha)]$ at the various sites α as a function of temperature. (a) is the case when $[Ca]=4 \times 10^{16} \text{ cm}^{-3}$ and (b) is the case when there is no Ca. A total $[H^+]=4 \times 10^{16} \text{ cm}^{-3}$ was assumed in the calculations.

frequencies of 3421 cm^{-1} for BC_{\parallel} and 3207 cm^{-1} for $Ca-AB_{O\perp}$ agree, within computational uncertainty, with the experimental lines at 3611 (Eagle-Picher) and 3326 cm^{-1} (Cermet). Note that although the absolute values here differ from experiments by about 100 – 200 cm^{-1} , the difference

between the two experimental modes of 3611 – $3326 = 285 \text{ cm}^{-1}$ is in a good agreement with that between the BC and AB_O configurations of 3421 – $3207 = 214 \text{ cm}^{-1}$. The BC_{\parallel} configuration has the oscillator oriented along the c axis, which is consistent with the experimental observation for the Eagle-Picher samples. The $Ca-AB_{O\perp}$ configuration has the oscillator orientated at 107° with respect to the c axis, which is consistent with the polarized IR measurement for the Cermet samples with transition moment aligned at 112° .

In conclusion, the large atomic-level spatial undulation of electric field makes the defect and impurity physics in ionic materials, in particular in ZnO , qualitatively different from that of covalent semiconductors. Larger than expected binding energy of 0.7 eV can result between charge neutral, isovalent Ca, and H^+ impurities. This tilts the energy balance between the BC and AB_O sites to favor $AB_{O\perp}$ in the presence of Ca. The calculated vibrational signatures of H^+ are also consistent with IR measurements. This may explain the current puzzle about the H^+ sites in ZnO .

This work was supported by NSFC (Contract No. 60525412), U.S. DOE/BES (Contract No. DE-AC36-99GO10337), JLU (start-up fund), CHE (CHE-RES-RG program), and AOARD/AFOSR (Contract No. FA4869-08-1-4007). We thank D. J. West, Z. G. Chen, X. Meng, H. Wang, D. Han, Q. D. Chen, and H. Yang for helpful discussions and technical supports.

*Corresponding author. sukit@sut.ac.th

- ¹C. G. Van de Walle, Phys. Rev. Lett. **85**, 1012 (2000).
- ²C. G. Van de Walle and J. Neugebauer, Nature (London) **423**, 626 (2003).
- ³K. Ip, M. E. Overberg, Y. W. Heo, D. P. Norton, S. J. Pearton, C. E. Stutz, B. Luo, F. Ren, D. C. Look, and J. M. Zavada, Appl. Phys. Lett. **82**, 385 (2003).
- ⁴S. J. Jokela and M. D. McCluskey, Phys. Rev. B **72**, 113201 (2005).
- ⁵E. V. Lavrov and J. Weber, Phys. Rev. B **73**, 035208 (2006).
- ⁶M. D. McCluskey, S. J. Jokela, K. K. Zhuravlev, P. J. Simpson, and K. G. Lynn, Appl. Phys. Lett. **81**, 3807 (2002).
- ⁷G. A. Shi, M. Stavola, S. J. Pearton, M. Thieme, E. V. Lavrov, and J. Weber, Phys. Rev. B **72**, 195211 (2005).
- ⁸K. Shimomura, K. Nishiyama, and R. Kadono, Phys. Rev. Lett. **89**, 255505 (2002).
- ⁹S. F. J. Cox, E. A. Davis, S. P. Cottrell, P. J. C. King, J. S. Lord, J. M. Gil, H. V. Alberto, R. C. Vilão, J. Piroto Duarte, N. Ayres de Campos, A. Weidinger, R. L. Lichti, and S. J. C. Irvine, Phys. Rev. Lett. **86**, 2601 (2001).
- ¹⁰C. H. Seager and S. M. Myers, J. Appl. Phys. **94**, 2888 (2003).
- ¹¹M. D. McCluskey and S. J. Jokela, *Proceedings of the NATO Advanced Workshop on Zinc Oxide*, NATO Science Series II: Mathematics, Physics, and Chemistry, Vol. 194, edited by N. Nickel and E. Terukov, (Springer, Dordrecht, 2005), p. 125.
- ¹²E. V. Lavrov, J. Weber, F. Börrnert, C. G. Van de Walle, and R. Helbig, Phys. Rev. B **66**, 165205 (2002).

¹³S. Limpijumnong and S. B. Zhang, Appl. Phys. Lett. **86**, 151910 (2005).

¹⁴M. D. McCluskey and S. J. Jokela, Physica B (Amsterdam) **401**–**402**, 355 (2007).

¹⁵D. C. Reynolds, C. W. Litton, D. C. Look, J. E. Hoelscher, B. Claflin, T. C. Collins, J. Nause, and B. Nemeth, J. Appl. Phys. **95**, 4802 (2004).

¹⁶R. Triboulet, V. Munoz-Sanjose, R. Tena-Zaera, M. C. Martinez-Tomas, and S. Hassani, *Proceedings of the NATO Advanced Workshop on Zinc Oxide*, NATO Science Series II: Mathematics, Physics, and Chemistry, Vol. 194, edited by N. Nickel and E. Terukov, (Springer, Dordrecht, 2005), p. 3.

¹⁷W. Kohn and L. J. Sham, Phys. Rev. **140**, A1133 (1965).

¹⁸P. E. Blöchl, Phys. Rev. B **50**, 17953 (1994).

¹⁹G. Kresse and D. Joubert, Phys. Rev. B **59**, 1758 (1999).

²⁰G. Kresse and J. Furthmüller, Phys. Rev. B **54**, 11169 (1996).

²¹G. Kresse and J. Furthmüller, Comput. Mater. Sci. **6**, 15 (1996).

²²E. McCartney, *Absorption and Emission by Atmospheric Gases: The Physical Processes* (Wiley, New York, 1983).

²³J. C. Phillips, Rev. Mod. Phys. **42**, 317 (1970).

²⁴R. F. W. Bader, *Atoms in Molecules: A Quantum Theory* (Oxford University Press, New York, 1994).

²⁵G. Henkelman, A. Arnaldsson, and H. Jonsson, Comput. Mater. Sci. **36**, 354 (2006).

²⁶A. F. Wright and S. M. Myers, J. Appl. Phys. **94**, 4918 (2003).

²⁷M. G. Wardle, J. P. Goss, and P. R. Briddon, Phys. Rev. Lett. **96**, 205504 (2006).